

Research Paper

# Biologically-Targeted Detection of Primary and Micro-Metastatic Ovarian Cancer

Tracy W. Liu<sup>†1</sup>, Jocelyn M. Stewart<sup>†1</sup>, Thomas D. MacDonald<sup>2</sup>, Juan Chen<sup>1</sup>, Blaise Clarke<sup>3</sup>, Jiyun Shi<sup>1,4</sup>, Brian C. Wilson<sup>1</sup>, Benjamin G. Neel<sup>1</sup>,  and Gang Zheng<sup>1</sup>, 

1. Department of Medical Biophysics, Princess Margarete Cancer Center, University of Toronto, Toronto, Canada;
2. Department of Pharmaceutical Sciences, University of Toronto, Toronto, Canada;
3. Department of Pathology, University Health Network, Toronto, Canada.
4. Medical Isotopes Research Center, Peking University, Beijing, China.

<sup>†</sup> Contributed equally to this work.

 Corresponding author: Benjamin G. Neel: [bneel@uhnres.utoronto.ca](mailto:bneel@uhnres.utoronto.ca) or Gang Zheng: [gang.zheng@uhnres.utoronto.ca](mailto:gang.zheng@uhnres.utoronto.ca).

© Ivyspring International Publisher. This is an open-access article distributed under the terms of the Creative Commons License (<http://creativecommons.org/licenses/by-nc-nd/3.0/>). Reproduction is permitted for personal, noncommercial use, provided that the article is in whole, unmodified, and properly cited.

Received: 2013.04.05; Accepted: 2013.05.03; Published: 2013.05.25

## Abstract

Ovarian cancer is the leading cause of morbidity/mortality from gynecologic malignancy. Early detection of disease is difficult due to the propensity for ovarian cancer to disseminate throughout the peritoneum. Currently, there is no single accurate test to detect primary or recurrent ovarian cancer. We report a novel clinical strategy using PPF: a multimodal, PET and optical, folate receptor (FR)-targeted agent for ovarian cancer imaging. The capabilities of PPF were evaluated in primary human ovarian cancer cells, *in vivo* xenografts derived from primary cells and *ex vivo* patient omentum, as the heterogeneity and phenotype displayed by patients is retained. Primary cells uptake PPF in a FR-dependent manner demonstrating approximately a 5- to 25-fold increase in fluorescence. By both PET and fluorescence imaging, PPF specifically delineated FR-positive, ovarian cancer xenografts, with similar tumor-to-background ratios of  $8.91 \pm 0.91$  and  $7.94 \pm 3.94$ , and micro-metastatic studding (<1mm), which demonstrated a 3.5-fold increase in PPF uptake over adjacent normal tissue. *Ex vivo* patient omentum demonstrated selective uptake of PPF by tumor deposits. The ability of PPF to identify metastatic deposits <1mm could facilitate more complete debulking (currently, optimal debulking is <10mm residual tumor), by providing a more sensitive imaging strategy improving treatment planning, response assessment and residual/recurrent disease detection. Therefore, PPF is a novel clinical imaging strategy that could substantially improve the prognosis of patients with ovarian cancer by allowing pre-, post- and intra-operative tumor monitoring, detection and possibly treatment throughout all stages of therapy and tumor progression.

Key words: Ovarian Cancer, Folate Receptor, PET, fluorescence imaging, multimodal.

## Introduction

Epithelial ovarian cancer is the leading cause of morbidity/mortality from gynecologic malignancy[1], with the high-grade serous ovarian cancer (SOC) histotype representing the largest proportion (65%) of cases[2]. SOC frequently presents at an advanced stage and has a poor overall survival, largely because the ovaries are located deep within the pelvis

and the disease presents with few persistent, and usually subtle, symptoms. Consequently, almost 90% of patients are diagnosed at Stage III/IV, with widespread peritoneal carcinomatosis, and a five-year survival of less than 30%[3]. Earlier detection of small volume disease, although essential for cure, is difficult with current modalities due to the propensity for per-

itoneal dissemination early in the course of disease. Most patients respond to current therapies, including cytoreductive surgery and chemotherapy. However, the majority (70-90%) of patients recur and eventually die of their disease[4]. Increased residual tumor volume after surgery increases the risk of relapse and decreases survival of SOC patients. Currently, there is no single accurate test to detect primary or recurrent disease. Therefore, methods that enhance the detection of SOC, before, during and after surgery, might improve the prognosis of patients with this deadly disease.

Several studies have revealed that up to 90% of human ovarian tumors, particularly those of the SOC subtype, overexpress folate receptor- $\alpha$  (FR)[5]. By contrast, most normal tissues express low to negligible levels of FR, raising the possibility that agents targeted to this receptor might be useful for imaging and/or drug delivery, in SOC and other FR-overexpressing tumors. Indeed, several studies have shown that folate can be used as a vehicle to deliver therapeutics or imaging agents directly to FR-overexpressing tumors[6-9]. Furthermore, one study demonstrated that a folate-targeted, single photon emission computed tomography (SPECT) imaging agent identified ovarian cancer patients who were more likely to benefit from folate-targeted therapy[9]. Recently, a folate-targeted, FITC-tagged small molecule for intraoperative FR-specific fluorescence imaging was reported[8]. Based on this evidence, FR has clinical potential as an imaging and therapeutic target for SOC. However, improvements to probe design that allow the use of multiple imaging modalities could increase the clinical applicability of FR-targeted agents.

Previously described folate receptor-targeted probes are either fluorescence- or SPECT-based[6-9]. However, positron emission tomography (PET) probes have multiple advantages, including: (1) shorter half-lives of most PET radioisotopes, allowing for faster clearance and higher dose administration; (2) ease of attenuation correction, producing better resolved images; (3) increased sensitivity (by 2-3 orders of magnitude), providing greater accuracy; and (4) wider clinical acceptance[10]. By contrast, PET lacks the ability to image patients in real-time with high resolution, generating increased interest in dual-modality imaging agents to aid in all stages of treatment management. For instance, by combining the non-invasive sensitivity of radionuclide imaging with the real-time, high sensitivity and high resolution of optical imaging, pre-operative and post-operative assessment of tumor burden by PET could initially be used to map disseminated lesions, and fluorescence imaging could then aid in im-

age-guided surgery to more precisely delineate tumor margins. Here we will demonstrate the first report of a dual, PET and optical, -targeted contrast agent with these capabilities for use as a novel clinical imaging strategy in ovarian cancer management.

Given the success of folate-targeted agents in the clinic, we targeted our multimodal PET/optical probe to the FR. This previously reported porphyrin-based probe (PPF) comprises 3 modules: (1) a multimodal porphyrin, Porphyrin- $\alpha$ , (2) a FR-homing molecule, folate, and (3) a pharmacomodulation peptide linker conjugating Pyro to Folate[11]. By exploiting the stable metal chelation capabilities of porphyrins, we previously demonstrated a simple and stable radiolabeling method for generating this  $^{64}\text{Cu}$ -PPF PET imaging probe[12]. In addition, we demonstrated the optical imaging and optical tuning capabilities of PPF, allowing tumor detection at multiple wavelengths[11, 13]. Herein, we report a novel clinical imaging strategy using the dual, PET and optical, FR targeted PPF for ovarian cancer management. We uniquely demonstrate that PPF can non-invasively delineate FR-positive, primary human SOC xenografts as well as micro-metastases in the peritoneum using both PET and fluorescence imaging modalities, potentially addressing the current clinical needs for SOC detection.

Early passage xenografts derived from primary SOC recapitulate the inter- and intra-patient heterogeneity observed in SOC[14], unlike cell line-derived xenografts[15]. Therefore, in this study we used either primary cells (freshly isolated from primary patient tumor samples) or xenografts derived from these cells. The clinical characteristics of the 31 patients from whom tissue was used are listed in Table 1.

**Table 1.** Patient characteristics of primary samples and xenografts.

Characteristic	Variable	Number (%)
Diagnosis*	Serous	30 (97)
	Undifferentiated	1 (3)
Age	Range	42-77
	Median	65.5
Stage	II	1 (3)
	III	17 (55)
	IV	3 (10)
	Unknown	10 (32)
Debulking Status	Optimal	13 (42)
	Sub-optimal	6 (19)
	Unknown	12 (39)
Chemotherapy Status	Naïve	13 (42)
	Neo-adjuvant	5 (16)
	Recurrence	13 (42)
Source of Cells	Solid tumor	19 (61)
	Ascites	12 (39)

\*All tumors used were high-grade.

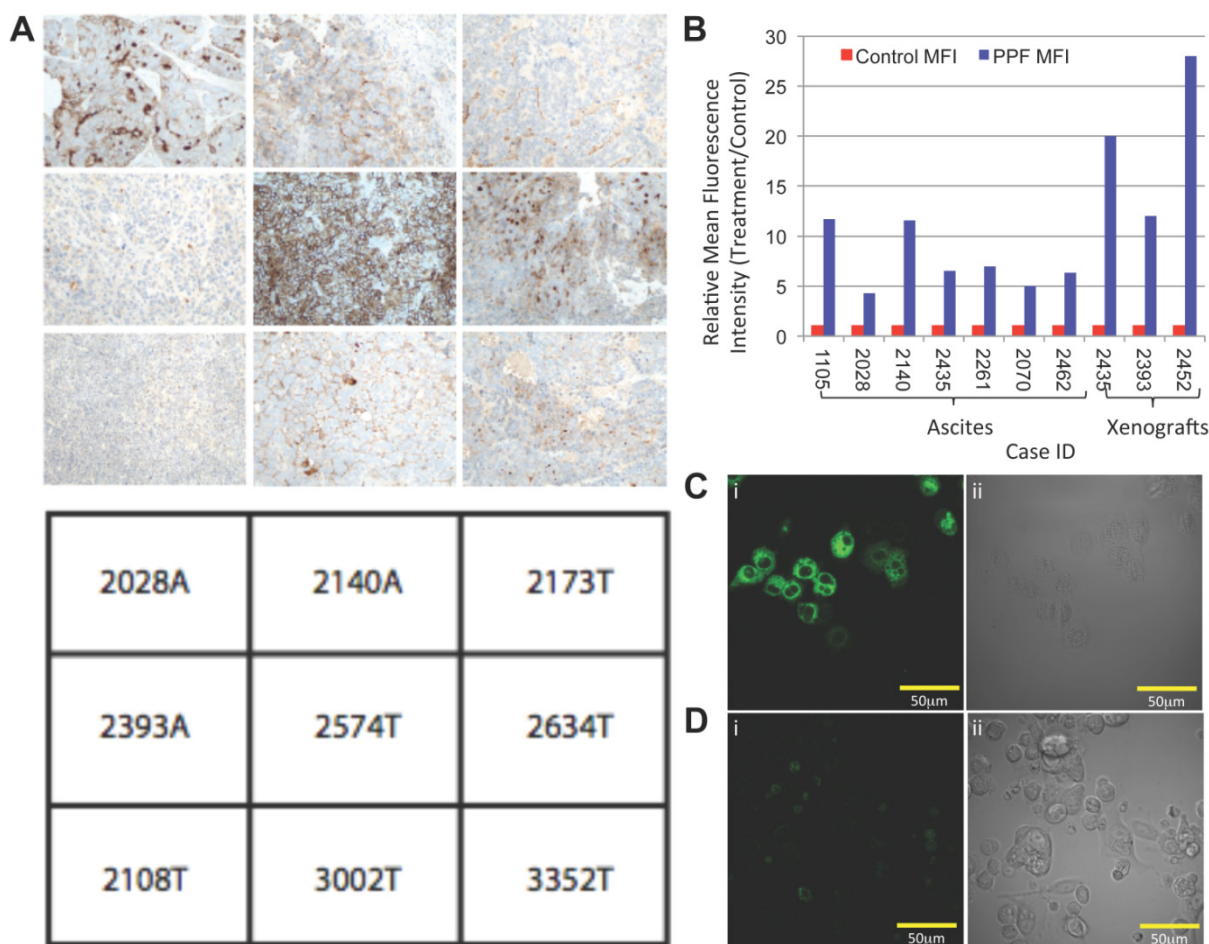


**Fig 1.** Folate receptor (FR) expression and function in primary ovarian cancer. (A) Immunohistochemical staining of FR expression in human tumor samples with corresponding sample IDs below. (B) *In vitro* PPF uptake by primary SOC cells, as assessed by flow cytometry. Data represent fold-change in mean fluorescence intensity after 1 h incubation with PPF. Representative confocal image of primary SOC cells after 3 h incubation of (C) 10  $\mu$ M PPF and (D) control; (i) PPF fluorescence and (ii) bright field image (Cells cultured in folate-free media for 5h prior to incubation with PPF, n=3 experimental replicates).

As expected from previous studies[5], immunohistochemical staining of a panel of early passage, primary human SOC xenografts revealed that most express FR $\alpha$  (Figure 1A), although the staining intensity and percentage of positive cells showed some variability. We used flow cytometry and confocal imaging to evaluate the uptake of PPF (50  $\mu$ M) by primary SOC and xenograft cells *ex vivo* [14]. In ascites (n=7) and xenograft (n=3) samples, the fluorescence intensity was 5- to 25-fold higher in cells incubated with PPF, compared with DMSO-treated control cells (Figure 1B, Supplementary Material: S1C), or cells incubated with PPF in the presence of excess folic acid (n=3, Supplementary Material: Figure S1A). Cell viability was unaffected by PPF exposure (Supplementary Material: Figure S1B). Likewise, cells incubated with PPF showed detectable intracellular fluorescence (Figure 1C) compared with control cells (without PPF, Figure 1D). Taken together, these observations confirm that primary human SOC cells take up PPF in a FR-dependent manner.

We used our established primary mammary fat

pad xenograft assay as a pre-clinical model to evaluate the *in vivo* imaging capability of PPF in multiple patient-derived samples (n=6).  $^{64}\text{Cu}$ -PPF distinguished SOC tumors from other tissues at 24 hours post injection (Supplementary Material: Figure S2). Although the highest uptake was observed in the kidneys and liver, the tumor-to-muscle ratio of  $^{64}\text{Cu}$ -PPF was  $4.97 \pm 0.61$  at 4 hours, and  $8.91 \pm 0.91$  at 24 hours, post-injection (Supplementary Material: Figure S2C), indicating rapid clearance of  $^{64}\text{Cu}$ -PPF from non-target tissues and probe retention in the tumor. This result was confirmed using fluorescence imaging as the tumor-to-muscle ratio of PPF at 24h was  $7.94 \pm 3.94$ . A strong fluorescence signal was localized within the tumor at 24h post-injection (Supplementary Material: Figure S2D), and was confirmed by confocal microscopy of frozen sections from these tumors (Supplementary Material: Figure S2E). To compare our PPF to the previously reported FR-targeted Fluorescein isothiocyanate (FITC) probe, we conjugated PPF to different fluorophores: FITC (PPF488), Pyropheophorbide- $\alpha$  (PPF) and Bacterio-

chlorophyll- $\alpha$  (PPF740), creating probes in the green, red and near infrared range, respectively (Supplementary Material: Figure S3). As expected, with increasing excitation wavelength, the tumor-to-background ratio increased, likely due to decreased auto-fluorescence and increased penetration depths of longer wavelengths of light (Supplementary Material: Figure S3C). These results demonstrate the capacity of PPF to image human SOC by either fluorescence or PET imaging.

Although mammary fat pad xenografts recapitulated the heterogeneity of SOC, they do not model other disease manifestations, such as peritoneal studding and ascites generation. Furthermore, the long imaging time point and unfavorable uptake within the abdomen after an intravenous injection is not ideal when trying to image SOC. Therefore, we also generated intraperitoneal xenografts from primary SOC, and tested the ability of PPF to accumulate in small metastases. In order to decrease the time between drug administration and imaging (1 hour), increase the drug concentration at target sites, and decrease

off-target accumulation, we administered PPF by a single intraperitoneal injection. A mixture of  $^{64}\text{Cu}$ -PPF (500 $\mu\text{Ci}$   $^{64}\text{Cu}$ , 6nmol of PPF) and PPF (2.25mg/kg, 30nmol PPF) was injected, and one hour later, the animals were imaged by PET/CT. A strong PET signal was evident in the abdominal cavities of animals with ascites, whereas healthy control mice showed no evident uptake of  $^{64}\text{Cu}$ -PPF (Figure 2A). Likewise, we could detect small metastatic studding (<1mm in size) on the peritoneal wall of animals with ascites by *in situ* fluorescent imaging after exposing the peritoneal cavity (Figure 2B&C). Fluorescence uptake into metastases was 3.5-fold higher than into adjacent normal tissue ( $p < 0.001$ ,  $n = 5$ ; Figure 2D). Fluorescence microscopy of frozen peritoneal slices also revealed the selectivity of PPF for malignant cells (Figure 2E). Histological analysis of serial H&E stained sections confirmed the presence of small, fluorescent deposits of malignant cells (Figure 2F). These results demonstrate the ability of PPF to identify animals with peritoneal spread of SOC by PET and fluorescence imaging.

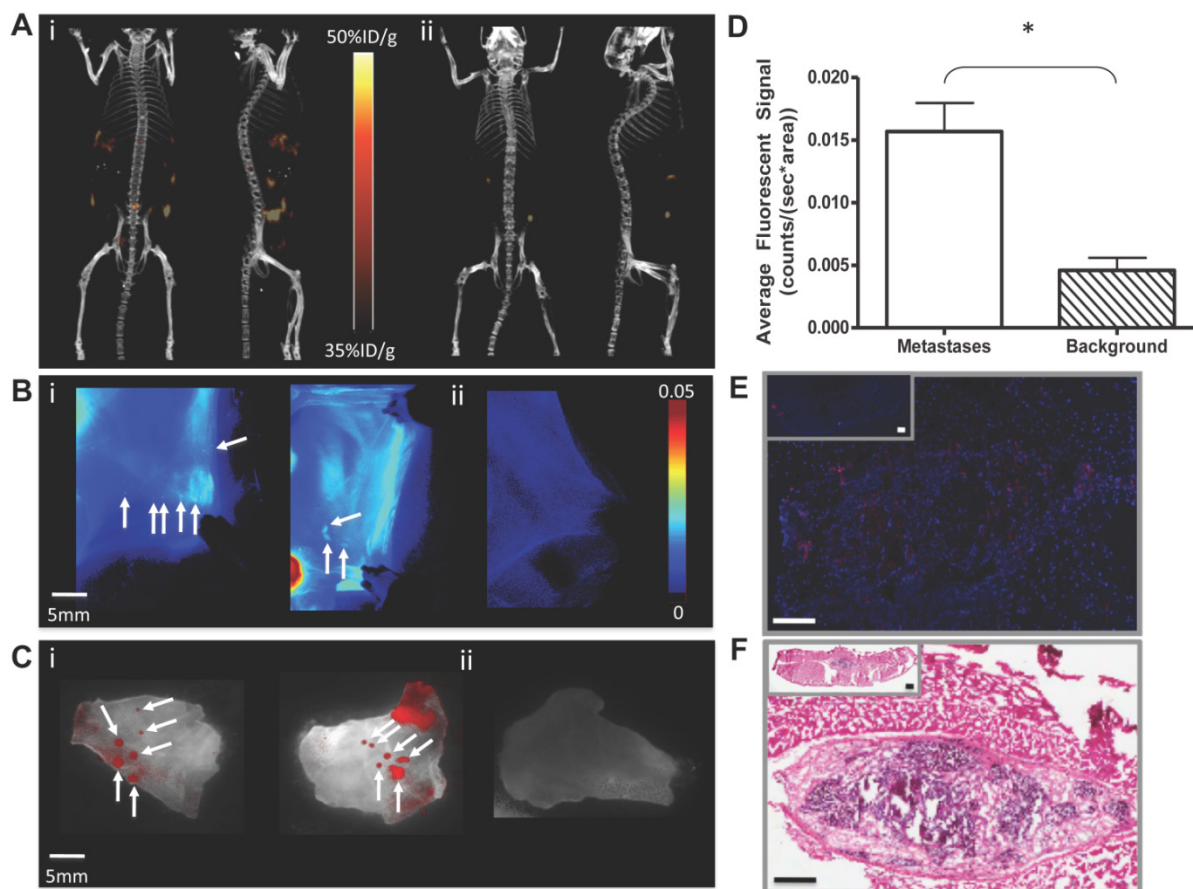


**Fig 2.** Tumor-specific uptake of PPF, measured by PET and fluorescent imaging in mouse ascites model. (A) Representative 3D PET/CT image of animals 1hr post-intraperitoneal injection of  $^{64}\text{Cu}$ PPF (500 $\mu\text{Ci}$ ) and PPF (2.25mg/kg), followed by (B) *in situ* composite fluorescent imaging of peritoneal cavity in: (i) ascites-bearing and (ii) control mice. (C) *Ex vivo* fluorescent imaging of peritoneal tissue in (i) ascites-bearing and (ii) control mice. White arrows depict small metastatic deposits in the peritoneum. (D) Average fluorescent signal of uptake of PPF versus background in micro-metastases. There is an approximately 3.5-fold increase in tumor to background ratio of PPF. Data are expressed as mean values  $\pm$  standard deviation ( $n = 5$ ); \*  $p < 0.001$ . (E) Histologic confirmation of PPF uptake and selectivity in micro-metastases. Frozen peritoneal slices (10 $\mu\text{m}$ ) were stained with DAPI (blue). Representative PPF fluorescence (red) images were compared to sequential (F) histology slices (H&E), confirming that fluorescent studding represents tumor foci. Full tissue slice is shown in inset; scale bars in (E) and (F) represent 500  $\mu\text{m}$ .

Finally, we evaluated the potential of PPF to be taken up by tumor deposits in the peritoneum *ex vivo*. Primary omentum from SOC patients (including tumor and adjacent normal tissue/stroma) was incubated in PPF (10 $\mu$ M). After 30 minutes, fluorescence was clearly detectable in the omentum (Figure 3A&B). Fluorescence microscopy of frozen omental slices again demonstrated selective uptake of PPF by cancer cells (Figure 3C), an assessment confirmed by histological analysis (Figure 3D). These data suggest that PPF also could be used intra-operatively to identify residual tumor during surgical debulking procedures.

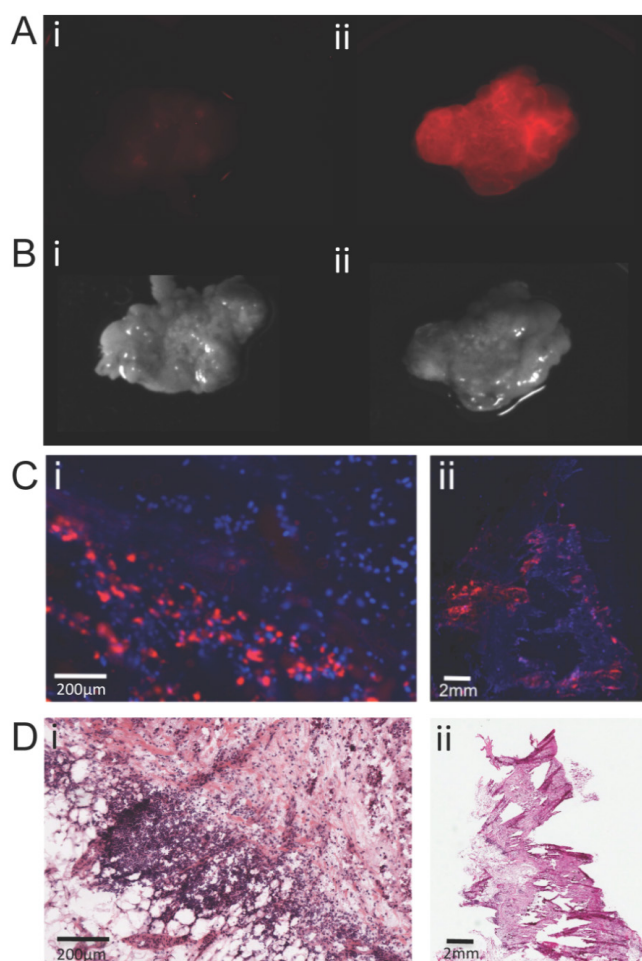


**Fig 3.** Uptake of PPF by primary human omentum from high-grade serous ovarian carcinoma patient. Imaging of human omentum by (A) fluorescence and (B) white light (i) before and (ii) 30 min after topical incubation with PPF (50 $\mu$ M). Corresponding representative (C) fluorescence (red) images were compared to sequential (D) H&E-stained slices of (i) magnified and (ii) full tissue slice, confirming microscopically the uptake and selectivity of PPF for cancerous cells. Frozen 10 $\mu$ m slices were DAPI-stained (blue). (Pyro excitation 410 $\pm$ 70 nm, detection 685 $\pm$ 40 nm).

## Discussion

Here, we report the application of a targeted, multimodal (PET/optical) probe for imaging ovarian cancer. We confirm the high specificity of PPF in primary human models of SOC (cell suspensions and xenografts). We demonstrate the ability of systemically or intraperitoneally injected PPF to clearly delineate FR-positive, primary human SOC xenografts, as well as bulk tumor and micro-metastatic studding in the peritoneum, using PET and fluorescence imaging. In addition, we validate the *ex vivo* uptake of PPF by metastatic deposits in primary human omentum, similar to a previous report showing the utility of a folate-targeted FITC probe[8]. PPF thus has the capacity to act as a "one size fits all" probe for detecting and monitoring SOC.

Primary human SOC cells and *in vivo* models derived from 31 patients were used for these studies because they retain the heterogeneity and phenotype that is displayed by patients[14]. Many studies of ovarian carcinogenesis, drug response and imaging efficacy have used immortalized cell lines that have been shown to poorly recapitulate the disease[15]. By using tumor cells derived from primary patient samples to evaluate the sensitivity of our multimodal PPF probe, we expect our results to better predict efficacy in SOC patients.

The value of PET[16-18] and optical imaging[19, 20] have been evaluated in ovarian cancer, although separately. Nevertheless, translation of such probes to the clinic requires the development of improved contrast agents to increase tumor sensitivity and specificity. Because FR is over-expressed in SOC, FR-targeted imaging and therapeutic agents have shown promise in clinical trials[6-9, 11] cementing FR as a viable molecular target in this disease. Two studies independently demonstrated the utility of FR-targeted probes, by SPECT or fluorescence, for identifying FR-positive ovarian cancer[8, 9]. These promising studies showed the clinical potential of FR-targeted imaging agents in SOC management; however, they highlighted a niche for a multi-modal agent. We have developed such an agent, PPF, whose appeal and novelty lie in its: (1) complementary imaging capabilities: specifically, the non-invasive, deep tissue penetration and quantitative nature of PET, combined with high-resolution, real-time fluorescence, ideal for surgical guidance; (2) targeted uptake, increasing the signal-to-noise ratio, and retention in tumors; and (3) applicability as a single agent, reducing concerns about variability in tumor uptake specificity, pharmacokinetics and pharmacodynamics.

PPF could aid the current clinical treatment strategy for ovarian cancer patients in several ways. As a PET agent, it could be used for staging pre- or post-operatively, allowing high-resolution evaluation of the extent of disease before and after treatment. Concomitantly, the fluorescence imaging properties of PPF could aid in image-guided surgery to precisely delineate tumor margins and/or residual disease. Optimal debulking (<10mm residual tumor) results in a significantly improved outcome for SOC patients[21], and patients with no detectable tumor at the time of resection demonstrate even greater survival[22]. The ability of PPF to identify metastatic deposits smaller than 1mm could facilitate more complete debulking than is possible currently. PPF also has potential as a disease-monitoring and recurrence-detection tool. Currently, CA125 allows detection of relapse approximately three months sooner than CT or MRI modalities[23], and combined with PET/CT, further expedites recurrence diagnosis[24]. At present, patients treated immediately upon biochemical relapse show no significant improvement in survival over those detected only when bulk disease recurs[23]. However, the current lack of benefit of detecting recurrence earlier most likely reflects the paucity of effective treatment options for relapsed disease. The future advent of new, targeted therapeutics and/or immunotherapies could make the diagnosis of smaller tumor bulk, not only important, but also essential. In turn, more sensitive imaging methods to improve treatment planning, response assessment and residual and/or recurrent disease detection will be needed. Moreover, 10-20% of SOC patients do not produce CA125, and at present, can only be monitored by radiologic methods [24, 25]. These patients also would benefit from more sensitive detection methods, including targeted PET and optical agents such as PPF.

Finally, it should be noted that Pyro is a potent photodynamic agent[11, 13]. Intraperitoneal PDT was evaluated in Phase II clinical trials, but did not demonstrate significant complete responses or long-term tumor control, with the ineffectiveness attributed to lack of tumor specificity in photosensitizer (Photofrin) uptake[26]. The high degree of tumor specificity of PPF might circumvent this limitation, by markedly reducing the risk of collateral damage to normal tissues within the peritoneum exposed to the photo-activating light. Studies evaluating the PDT potential of PPF are currently underway. Thus, in addition to its utility as an imaging agent, PPF might aid in the eradication of residual intraperitoneal tumor and microscopic metastatic deposits by applying a tumor-targeted PDT treatment to the entire surgical

bed post-resection.

Taken together, our results demonstrate that PPF is an "all-in-one" novel clinical imaging strategy that could substantially improve the prognosis of patients with SOC and other malignancies over-expressing FR, such as endometrial cancer and colon cancer, by allowing pre-, post- and intra-operative tumor monitoring, detection and possibly also treatment throughout all stages of therapy and tumor progression.

## Materials and Methods

**Tumor Samples and Cells:** High-grade SOC samples were obtained from the University Health Network Tissue Bank with patient consent and Research Ethics Board approval, and were pathologist-verified. Tumors were procured within 2-4 h of excision. Samples were processed as reported previously [14]. Briefly, solid tumors were minced and digested with collagenase/hyaluronidase (Stem Cell Technologies) in DMEM at 37 °C for 2 h. Red blood cells were lysed in 0.16 M ammonium chloride, and the remaining cells were filtered through a 70- $\mu$ m mesh and counted. Ascites cells were collected by centrifugation at 300xg and red blood cells lysed as above. Cells can be revived and form tumors after viable freezing [14].

**Xenografts:** All animal studies were carried out under institutional approval (University Health Network, Toronto, Canada). CD45-depleted cells ( $10^6$ ) in 1:1 HBSS:growth factor-reduced Matrigel (BD Biosciences) were injected into the mammary fat pad (xenograft model) or peritoneum (ascites model) of Non-Obese Diabetic/Severe Combined Immunodeficient (NOD/SCID) or NOD/SCID/Il2r $\gamma^{-/-}$  (NSG) mice. Mice were monitored for tumors for up to 6 months post-injection or until moribund. After euthanization, tumors and tissues were harvested for subsequent histology and/or biodistribution studies.

**MicroPET/CT Imaging:** MicroPET imaging was performed with a Siemens Focus 220 MicroPET scanner (Siemens, Munich, Germany). Tumor-bearing mice were anesthetized with 2% isoflurane in oxygen, injected with ~500 $\mu$ Ci of  $^{64}$ Cu-PPF (6nmol of PPF) via their tail veins, and placed near the center of the field of view, where the highest resolution and sensitivity are obtained. A 10 minute static PET image was obtained at 4 h post-injection, and 30-45 min. static PET images were acquired at 24 h post-injection. CT scans were obtained immediately after each PET imaging session. To this end, mice remained anesthetized throughout PET imaging, and then were transferred without any movement directly to a GE Locus Ultra microCT scanner (GE Healthcare, Little Chalfont,

UK), together with the supporting bed.

**Biodistribution studies:** Biodistribution studies were performed using NOD/SCID mice bearing primary human SOC xenografts in the mammary fat pad. The  $^{64}\text{Cu}$  radiotracer ( $\sim 500 \mu\text{Ci}$  in 0.1 mL saline) was administered into each animal via the tail vein. Animals were euthanized 4 or 24 h post-injection with 2% isoflurane, and exsanguinated by opening the thoracic cavity and withdrawing blood samples from the heart using a syringe. Organs were excised, washed with saline, dried with absorbent tissue, weighed and counted on a  $\gamma$ -counter (Perkin-Elmer Wizard-1480). Organs examined included the tumor, heart, spleen, lungs, liver, kidneys, adrenal, stomach, intestine, muscle, bone and brain. Organ uptake was calculated as percentage of the injected dose per gram of tissue (%ID/g). Biodistribution data and target-to-background (T/B) ratios are reported as the mean and standard deviation based on results from three animals at each time point. Comparisons between radiotracers were made using the two-way ANOVA test (GraphPad Prim 5.0, San Diego, CA). The level of significance was set at  $p < 0.05$ .

**Optical imaging studies:** A solution of 2.25 mg/kg of PPF (30nmol of PPF) was formulated in 150  $\mu\text{L}$  of an aqueous solution containing 5  $\mu\text{L}$  of DMSO and 1.5  $\mu\text{L}$  of Tween80. When tumors reached 5-10 mm in diameter, mice were injected with the PPF solution intravenously via their tail veins under isoflurane anesthesia. Whole-body *in vivo* fluorescent imaging was performed before and at multiple time points (30 min, 2h, 6.5h and 24h) after injection using the MaestroTM, CRi: PPF - 661 nm (641 to 681 nm) excitation, 700nm longpass detection.

**Ascites imaging studies:** In order to reduce absorption by the cellular fraction of the ascites, fluid (0.5-1mL/animal) was drained from the abdominal cavity of tumor-bearing mice using a 27G needle before injection and imaging. A mixture of  $^{64}\text{Cu}$ -PPF and PPF was administered intraperitoneally to animals with ascites and healthy controls. PET/CT images were captured over 10 minutes at 1hr post-injection. Animals were then euthanized, and *ex vivo* fluorescence imaging of the peritoneal cavity was performed (MaestroTM, CRi: PPF - 680nm excitation, 700nm longpass detection, auto-exposure integration time, total fluorescence signals normalized by exposure time and ROI area (total signal/(ms \* pixels)). Comparisons between small metastatic deposits and background signals were made using the two-sample homoscedastic student t-test, with the level of significance set at  $p < 0.05$ .

**Omentum optical imaging:** Omental samples were imaged prior to incubation with PPF (10 $\mu\text{M}$ ) at

37°C. *Ex vivo* fluorescence imaging was performed at multiple time points (30min, 1h, 2h, 4h, 5.5h and 24h), similar to the *in vivo* optical imaging protocol reported above. At 24h, the omentum was snap-frozen in liquid nitrogen with OCT media and stored at -80°C. Frozen sections (10 $\mu\text{m}$ ) were cut on a cryostat. Frozen tissue slices were immersed in PBS for 5 min, dried, and 10 $\mu\text{L}$  of mounting solution with DAPI (Vector laboratories, Inc.) were added as a nuclear stain. Sections were overlaid with coverslips and imaged (Olympus Upright Tiling Microscope, BX50; excitation 410 $\pm$ 70nm, emission 685 $\pm$ 40nm). A section adjacent to the imaged frozen section was stained with Hematoxylin & Eosin (H&E) to confirm the presence of peritoneal carcinomatosis.

## Supplementary Material

Fig.S1 - S3. <http://www.thno.org/v03p0420s1.pdf>

## Acknowledgements

Funding was provided by Canadian Institute for Health Research (GZ), Princess Margaret Hospital Foundation (GZ/BN), Joey and Toby Tanenbam/Brazilian Ball Chair in Prostate Cancer Research (GZ), Terry Fox Foundation (Canadian Cancer Society Research Institute - Terry Fox Program Project Grant 020003, BN), Samuel Waxman Cancer Research Foundation (BN), Canadian Graduate Scholarship - Canadian Institute for Health research CIHR-CGS-200710MDR (JS) and Department of Defense BCRP Predoctoral Award W81XWH-10-1-0115 (TL).

## Competing Interests

The authors have declared that no competing interest exists.

## References

1. Committee CCsS. Statistics for ovarian cancer. Canadian Cancer Encyclopedica from Canadian Cancer Society. 2010.
2. Prat J. Ovarian carcinomas: five distinct diseases with different origins, genetic alterations, and clinicopathological features. *Virchows Arch.* 2012; 460: 237-49. doi:10.1007/s00428-012-1203-5.
3. Clarke-Pearson DL. Clinical practice. Screening for ovarian cancer. *N Engl J Med.* 2009; 361: 170-7. doi:361/2/170 [pii] 10.1056/NEJMcp0901926.
4. Naumann RW, Coleman RL. Management strategies for recurrent platinum-resistant ovarian cancer. *Drugs.* 2011; 71: 1397-412. doi:10.2165/11591720-000000000-00000.
5. Kalli KR, Oberg AL, Keeney GL, Christianson TJ, Low PS, Knutson KL, et al. Folate receptor alpha as a tumor target in epithelial ovarian cancer. *Gynecologic oncology.* 2008; 108: 619-26. doi:10.1016/j.ygyno.2007.11.020.
6. Siegel BA, Dehdashti F, Mutch DG, Podoloff DA, Wendt R, Sutton GP, et al. Evaluation of  $^{111}\text{In}$ -DTPA-folate as a receptor-targeted diagnostic agent for ovarian cancer: initial clinical results. *Journal of nuclear medicine : official publication, Society of Nuclear Medicine.* 2003; 44: 700-7.
7. White RLC AJ, Armstrong DK, Glenn D, et al. Efficacy and safety of farletuzumab, a humanized monoclonal antibody to folate receptor

- alpha, in platinum-sensitive relapsed ovarian cancer subjects: Final data from a multicenter phase II study [abstract no 5001]. *J Clin Oncol*. 2010; 28.
8. van Dam GM, Themelis G, Crane LM, Harlaar NJ, Pleijhuis RG, Kelder W, et al. Intraoperative tumor-specific fluorescence imaging in ovarian cancer by folate receptor-alpha targeting: first in-human results. *Nature medicine*. 2011; 17: 1315-9. doi:10.1038/nm.2472.
  9. Symanowski JT, Maurer AH, Naumann RW, Shah NP, Morgenstern D, Messmann RA. Use of <sup>99m</sup>Tc-EC20 (a folate-targeted imaging agent) to predict response to therapy with EC145 (folate-targeted therapy) in advanced ovarian cancer. *ASCO Meeting Abstracts*. 2010; 28: 5034.
  10. Rahmim A, Zaidi H. PET versus SPECT: strengths, limitations and challenges. *Nuclear medicine communications*. 2008; 29: 193-207. doi:10.1097/MNM.0b013e3282f3a515.
  11. Stefflova K, Li H, Chen J, Zheng G. Peptide-based pharmacomodulation of a cancer-targeted optical imaging and photodynamic therapy agent. *Bioconjug Chem*. 2007; 18: 379-88. doi:10.1021/bc0602578.
  12. Shi J, Liu TW, Chen J, Green D, Jaffray D, Wilson BC, et al. Transforming a targeted porphyrin theranostic agent into a PET imaging probe for cancer. *Theranostics*. 2011; 1: 363-70.
  13. Liu TW, Chen J, Burgess L, Cao W, Shi J, Wilson BC, et al. Multimodal bacteriochlorophyll theranostic agent. *Theranostics*. 2011; 1: 354-62.
  14. Stewart JM, Shaw PA, Gedye C, Bernardini MQ, Neel BG, Ailles LE. Phenotypic heterogeneity and instability of human ovarian tumor-initiating cells. *Proc Natl Acad Sci U S A*. 2011; 108: 6468-73. doi:10.1073/pnas.1005529108.
  15. Shaw TJ, Senterman MK, Dawson K, Crane CA, Vanderhyden BC. Characterization of intraperitoneal, orthotopic, and metastatic xenograft models of human ovarian cancer. *Mol Ther*. 2004; 10: 1032-42. doi:10.1016/j.ymthe.2004.08.013.
  16. Kyriazi S, Kaye SB, deSouza NM. Imaging ovarian cancer and peritoneal metastases—current and emerging techniques. *Nature reviews Clinical oncology*. 2010; 7: 381-93. doi:10.1038/nrclinonc.2010.47.
  17. Prakash P, Cronin CG, Blake MA. Role of PET/CT in ovarian cancer. *AJR American journal of roentgenology*. 2010; 194: W464-70. doi:10.2214/AJR.09.3843.
  18. Musto A, Rampin L, Nanni C, Marzola MC, Fanti S, Rubello D. Present and future of PET and PET/CT in gynaecologic malignancies. *European journal of radiology*. 2011; 78: 12-20. doi:10.1016/j.ejrad.2009.12.035.
  19. Crane LM, van Oosten M, Pleijhuis RG, Motekallemi A, Dowdy SC, Cliby WA, et al. Intraoperative imaging in ovarian cancer: fact or fiction? *Molecular imaging*. 2011; 10: 248-57. doi:10.2310/7290.2011.00004.
  20. Sheth RA, Upadhyay R, Stangenberg L, Sheth R, Weissleder R, Mahmood U. Improved detection of ovarian cancer metastases by intraoperative quantitative fluorescence protease imaging in a pre-clinical model. *Gynecologic oncology*. 2009; 112: 616-22. doi:10.1016/j.ygyno.2008.11.018.
  21. Bast RC, Jr., Hennessy B, Mills GB. The biology of ovarian cancer: new opportunities for translation. *Nature reviews Cancer*. 2009; 9: 415-28. doi:10.1038/nrc2644.
  22. Hyman DM, Long KC, Tanner EJ, Grisham RN, Arnold AG, Bhatia J, et al. Outcomes of primary surgical cytoreduction in patients with BRCA-associated high-grade serous ovarian carcinoma. *Gynecologic oncology*. 2012; 126: 224-8. doi:10.1016/j.ygyno.2012.05.001.
  23. Rustin GJ, van der Burg ME, Griffin CL, Guthrie D, Lamont A, Jayson GC, et al. Early versus delayed treatment of relapsed ovarian cancer (MRC OV05/EORTC 55955): a randomised trial. *Lancet*. 2010; 376: 1155-63. doi:10.1016/S0140-6736(10)61268-8.
  24. Gu P, Pan LL, Wu SQ, Sun L, Huang G. CA 125, PET alone, PET-CT, CT and MRI in diagnosing recurrent ovarian carcinoma: a systematic review and meta-analysis. *European journal of radiology*. 2009; 71: 164-74. doi:10.1016/j.ejrad.2008.02.019.
  25. Bast RC, Jr., Klug TL, St John E, Jenison E, Niloff JM, Lazarus H, et al. A radioimmunoassay using a monoclonal antibody to monitor the course of epithelial ovarian cancer. *The New England journal of medicine*. 1983; 309: 883-7. doi:10.1056/NEJM198310133091503.
  26. Hahn SM, Fraker DL, Mick R, Metz J, Busch TM, Smith D, et al. A phase II trial of intraperitoneal photodynamic therapy for patients with peritoneal carcinomatosis and sarcomatosis. *Clinical cancer research : an official journal of the American Association for Cancer Research*. 2006; 12: 2517-25. doi:10.1158/1078-0432.CCR-05-1625.